

Leveraging Disease Progression Learning for Medical Image Recognition

Qicheng Lao and Thomas Fevens

Department of Computer Science and Software Engineering,
Concordia University, Montréal, QC, Canada
{qi_lao, fevens}@encs.concordia.ca

Abstract. Unlike natural images, medical images often have intrinsic characteristics that can be leveraged for neural network learning. For example, images that belong to different stages of a disease may continuously follow certain progression pattern. In this paper, we propose a novel method that leverages disease progression learning for medical image recognition, where sequences of images ordered by disease stages are learned by a neural network that consists of a shared vision model for feature extraction and a long short-term memory network for the learning of stage sequences. Auxiliary vision outputs are also included to capture stage features that tend to be discrete along disease progression. Our proposed method is evaluated on a diabetic retinopathy dataset, and achieves about 3.3% improvement in disease staging accuracy, compared to the baseline method that does not use disease progression learning.

1 Introduction

Deep learning has been widely applied to medical image recognition since its great success in natural image recognition, and has achieved state-of-the-art performance in various areas such as lesion detection and classification [1]. Unlike general object classification, medical images often have intrinsic characteristics that can be exploited to facilitate neural network learning for optimal results. For example, medical recognition tasks on images acquired from computed tomography (CT) or magnetic resonance imaging (MRI) generally favor 3D convolutional neural network (CNN) over 2D CNN, due to the additional spatial information in three dimensions [2]. Another example of neural networks that exploit medical intrinsic information is the BrainNetCNN, where special edge-to-edge, edge-to-node and node-to-graph convolutional filters are designed to leverage topological locality of brain networks for the prediction of neurodevelopmental outcomes [3].

In this paper, we propose a novel method that leverages disease progression learning for medical image recognition. Concretely, given any medical recognition problem that is associated with a disease progression, we use long short-term memory (LSTM) to model the disease progression, for example, to predict survival time based on brain tumor images (e.g. short-term survival, medium-term survival and long-term survival) [4], or a disease staging problem. As illustrated

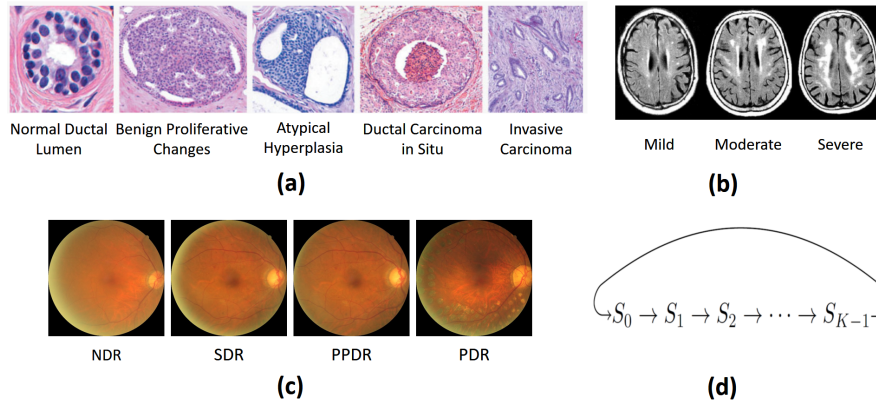


Fig. 1. Examples of disease progression with different stages: (a) Breast cancer [5]; (b) Aging [6]; (c) Diabetic retinopathy [7]; (d) Cyclic form of the stage sequence.

in Figure 1(a, b, c), the disease staging problem commonly exists across multiple modalities, including but not limited to classifying breast histopathological images into normal, benign, in-situ or invasive; MRI images of white matter into mild, moderate or severe; and retinal fundus images into no-diabetic-retinopathy (NDR), simple-diabetic-retinopathy (SDR), pre-proliferative-diabetic-retinopathy (PPDR) or proliferative-diabetic-retinopathy (PDR). Rather than considering each different stage as an independent class as done in most previous research, we hypothesize that there is a stage difference memory driven by the disease progression that should also be represented in the neural network. By leveraging this memory information from stage sequence, more robust and optimal results could be possible.

LSTM is a widely-used network that is powerful for sequential data learning, as it has memory units that efficiently remember previous steps [8]. There are previous publications using LSTM for medical data, but mostly based on diagnostic text reports [9], clinical measurements/admissions [10–12], or 3D image stacks [13, 14], among which, some also use the concept of disease progression modeling [11, 12]. However, all previous work either do not clearly define stage classes for a disease progression, or still consider each stage as an independent class and the sequence learning only occurs inside each individual stage class. I.e., there is no explicit learning of the stage sequence itself, other than learning of temporal sequence (e.g. a series of clinical events), or spatial sequence (e.g. 3D MRI/CT images).

To the best of our knowledge, we are the first to use LSTM for the learning of stage sequence along the disease progression for medical image recognition, with each stage represented by feature vectors that are extracted from a well-established vision model (e.g. GoogleNet or ResNet). Auxiliary outputs from the vision model are also adopted in order to capture stage features that may not be continuous along the disease progression. Our proposed method is evaluated

on a diabetic retinopathy dataset, where it shows a performance increase of around 3.3% in disease staging accuracy, compared to the baseline method that is without disease progression learning.

2 Methods

2.1 Disease progression learning

Given a disease progression with K sequential stages $S = \{S_k, k = 0, 1, \dots, K-1\}$, with $S_k > S_{k-1}$ for each $k \in (0, K-1]$, where the greater-than sign indicates a disease progression, meaning stage S_k is a subsequent stage of S_{k-1} , e.g. $\{NDR, SDR, PPDR, PDR\}$ for diabetic retinopathy and $\{normal, benign, in-situ, malignant\}$ for epithelial cancers, we want the neural network to learn disease stage progression by presenting it with a sequence of images ordered by disease stage as the input $\mathbf{x} = [I^{S_0}, I^{S_1}, \dots, I^{S_{K-1}}]$, where I^{S_k} is a randomly selected image that belongs to stage S_k , and the corresponding output is simply the ordered full sequence of all disease stages: $\mathbf{y} = [S_0, S_1, \dots, S_{K-1}]$. However, with the above design, all the input samples would share the same output \mathbf{y} that is fixed by the disease stage progression, making the network training meaningless. To overcome this problem, we artificially define $S_0 > S_{K-1}$ to make the stage sequence cyclic (Figure 1(d)), so that multiple ordered full sequences of all disease stages can be generated. Therefore, $[S_1, S_2, \dots, S_{K-1}, S_0]$, for example, is also considered as a valid ordered full sequence containing all stages for a certain disease. As a result, the notation of stage sequence for a training sample can be updated more formally as the following:

$$(\mathbf{x}, \mathbf{y}) = ([I^{S_{i+0 \pmod{K}}}, I^{S_{i+1 \pmod{K}}}, \dots, I^{S_{i+K-1 \pmod{K}}}], [S_{i+0 \pmod{K}}, S_{i+1 \pmod{K}}, \dots, S_{i+K-1 \pmod{K}}]) \quad (1)$$

where $i \in [0, K-1]$ is the step shift size and K is the total number of disease stages. For simplicity of notation and explanation, we use stage sequence of $i = 0$ as an illustration in the following.

As shown in Figure 2, the proposed method contains a vision model (e.g. GoogleNet or ResNet) for the feature extraction, followed by a LSTM model for the purpose of disease progression learning. The vision model extracts a feature vector $\mathbf{z}^{S_k} \in \mathbb{R}^C$ from its belonging input image I^{S_k} for each disease stage S_k , and the concatenated feature vector sequence of all stages $\mathbf{z} = [\mathbf{z}^{S_0}, \mathbf{z}^{S_1}, \dots, \mathbf{z}^{S_{K-1}}] \in \mathbb{R}^{K \times C}$ is given as the input to LSTM. The LSTM maintains a hidden state $\mathbf{h}^{S_k} \in \mathbb{R}^G$ and a cell state $\mathbf{c}^{S_k} \in \mathbb{R}^G$, which are updated at each stage step $k \in (0, K-1]$:

$$\mathbf{h}^{S_k}, \mathbf{c}^{S_k} = \text{LSTM}(\mathbf{z}^{S_k}, \mathbf{h}^{S_{k-1}}, \mathbf{c}^{S_{k-1}}) \quad (2)$$

The hidden state sequence of all stages $\mathbf{h} = [\mathbf{h}^{S_0}, \mathbf{h}^{S_1}, \dots, \mathbf{h}^{S_{K-1}}] \in \mathbb{R}^{K \times G}$ is collected to learn a softmax classifier \mathcal{F} on top of LSTM model, which outputs the hypotheses $\hat{\mathbf{y}}$ of the true stage labels \mathbf{y} :

$$\hat{\mathbf{y}} = \mathcal{F}(\mathbf{h}; \boldsymbol{\theta}) \quad (3)$$

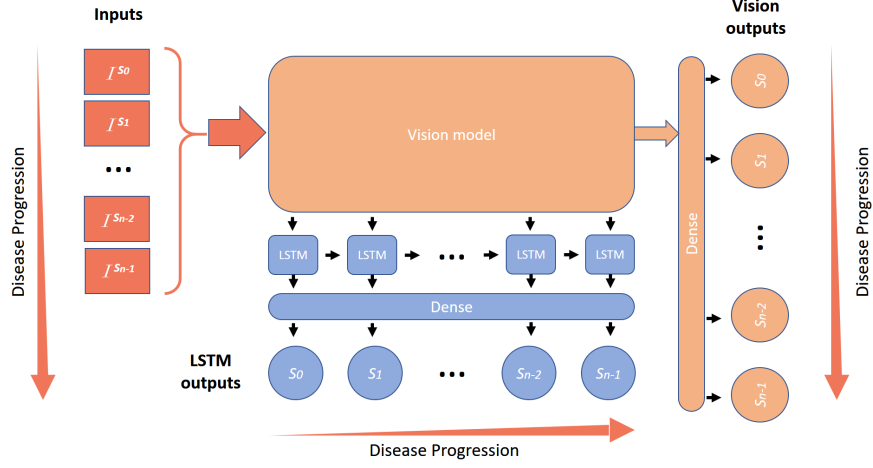


Fig. 2. The architecture of our proposed network.

where θ is the parameter for classifier \mathcal{F} . Note that $\hat{\mathbf{y}} = [\hat{\mathbf{y}}^{S_0}, \hat{\mathbf{y}}^{S_1}, \dots, \hat{\mathbf{y}}^{S_{K-1}}] \in \mathbb{R}^{K \times K}$, where each sequence element represents a probability distribution over K stage labels for its corresponding stage.

Our loss function is a weighted summation of cross entropy losses at all stages:

$$Loss(\hat{\mathbf{y}}, \mathbf{y}) = \sum_{k=0}^{K-1} \alpha_k \cdot l(\hat{\mathbf{y}}^{S_k}, S_k) \quad (4)$$

where α_k is the loss weight for each stage output and

$$l(\hat{\mathbf{y}}^{S_k}, S_k) = \sum_{j=0}^{K-1} -\log \hat{y}_j^{S_k} \cdot \delta(S_k = S_j) \quad (5)$$

is the cross entropy loss function, with $\hat{y}_j^{S_k}$ denoting for the probability value of image I^{S_k} belonging to the stage label S_j .

2.2 Auxiliary vision outputs

In addition to disease progression learning, the network should also be able to capture discriminative features that tend to be discrete among different stages along the disease progression, e.g. features that only appear in a certain disease stage. Given this thought, we also design auxiliary outputs directly from the vision model extracted features \mathbf{z} with another softmax classifier \mathcal{F}_v on top of the vision model:

$$\hat{\mathbf{y}}_v = \mathcal{F}_v(\mathbf{z}; \theta_v) \quad (6)$$

To distinguish the two classifiers on top of LSTM model (\mathcal{F}_l) and vision model (\mathcal{F}_v), Equation (3) is updated as:

$$\hat{\mathbf{y}}_l = \mathcal{F}_l(\mathbf{h}; \boldsymbol{\theta}_l) \quad (7)$$

Similarly to LSTM outputs, the loss for auxiliary vision outputs is also defined as the weighted summation of cross entropy losses at all disease stages. Taking both losses into account, the final loss function for our proposed network is:

$$Loss(\hat{\mathbf{y}}_l, \hat{\mathbf{y}}_v, \mathbf{y}) = \sum_{k=0}^{K-1} (\alpha_k \cdot l(\hat{\mathbf{y}}_l^{S_k}, S_k) + \beta_k \cdot l(\hat{\mathbf{y}}_v^{S_k}, S_k)) \quad (8)$$

The loss weights α_k and β_k for each stage should be chosen depending on each individual disease progression. A heuristic choice is that more weight should be given to β_k if the stage features tend to be more discrete.

2.3 Testing phase

In the testing phase, given an image I_{test} , an artificial image sequence is generated by repeating I_{test} for K iterations, and then the sequence is fed into the trained network. Due to the design of our network, we have two options to predict its stage label based on either LSTM output $\hat{\mathbf{y}}_l$ or vision output $\hat{\mathbf{y}}_v$ (see Figure 2). In both cases, only the first stage output in the sequence is reported as the final predicted label. Note that the input image sequence can be started with any arbitrary stage as we described earlier in Section 2.1. Therefore a faked sequence starting with I_{test} can still result in a reasonable prediction of stage label for I_{test} based on its corresponding first stage output, although the rest stage outputs are invalid since there is no disease progression in the input sequence.

2.4 Baseline network

The baseline network for this study is the same vision model followed by the same softmax classifier \mathcal{F}_v as used in our proposed network, except that the input is a single image, similar to most previous research work on medical image classification.

For a fair comparison, we also make sure that both networks are trained on exactly the same amount of augmented data, which we will describe in detail in Section 3.2, to rule out the possibility that a superior performance could be gained simply due to larger training samples, given the fact that the input size of our proposed network is $K - 1$ times bigger than that of the baseline network.

3 Experiments and Results

3.1 Dataset

To evaluate our proposed network, we choose to use a recently published dataset on diabetic retinopathy [7], which contains fundus photographs of four stages.

The dataset has two sets of class labels based on whether to grade with wider retinal area: Davis grading of one figure and Davis grading of concatenated figures, and we use the former in our experiments. There are in total 9939 images, with 6561 of NDR, 2113 of SDR, 460 of PPDR and 805 of PDR.

Unlike previous work [7], we address the data imbalance problem by under-sampling by a random selection of 460 images from each stage class for each independent experiment, and moreover, all the images are resized to 200×200 instead of 1272×1272 to speed up training, since it is not our purpose here to compete with the result in [7], but rather to investigate the advantage of disease progression learning in stage classification.

Out of the final resulting dataset, 10% of the data is randomly reserved for testing, and the rest is further split into two parts: 90% for training and 10% for validation. Data augmentation is performed on the training set by only using random rotations from -5° to 5° without shifts or flips, as all the images share the same position.

3.2 Implementation details

We examine two types of vision models in our experiments: GoogleNet and ResNet-50, both of which were pretrained on ImageNet. The freeze layer is set to 64 for GoogleNet and 36 for ResNet-50. We use $C = 256$ for the dimension of extracted feature vectors, $G = 256$ for the LSTM model and $\alpha = \beta = \mathbf{1} \in \mathbb{R}^K$. All models are implemented in Keras with Theano backend, and trained using stochastic gradient descent, with the initial learning rate set to 0.001, decay by $1e-6$ over each update, and Nesterov momentum is set to 0.9.

For each independent experiment, we evaluate the proposed network and baseline network on the same random split of the dataset. We repeat the above comparison experiment for 20-30 times, each with a different split. To make sure both networks are trained on the same amount of augmented data, the same number of iteration steps per epoch (i.e. 100 steps and 500 steps) is used in the training, until the validation loss does not drop for ten epochs (patience = 10, with the maximum number of epochs set to 100). In order to compensate the input size difference (i.e. one-image input against four-image input), the batch size for the baseline network training is set to 64 and decreased to 16 for our proposed network. Note that this is the only difference in hyper-parameter settings for the training of the two networks.

3.3 Results

Table 1 shows the performance comparison of our proposed method and the baseline method, with both results of GoogleNet Inception v3 and ResNet-50 as the vision model. As is shown in the table, our proposed method outperforms the baseline across all experimental settings that are used in this paper (choices of vision model and training steps per epoch), and on average, there is about 3.3% accuracy gain (2.4%, 3.6%, 3.4% and 3.6% for each setting respectively). However, we do not observe a significant performance difference between vision

Table 1. Performance comparisons of the baseline method and our proposed method (with both vision outputs and LSTM outputs).

Vision model	Steps ^a	Method	Accuracy
GoogleNet Inception v3	100	BASELINE	57.0 ± 3.2%
		Ours(VISION OUTPUT)	59.4 ± 3.1%
		Ours(LSTM OUTPUT)	59.2 ± 3.3%
	500	BASELINE	59.5 ± 3.3%
		Ours(VISION OUTPUT)	63.1 ± 2.7%
		Ours(LSTM OUTPUT)	62.9 ± 3.0%
ResNet-50	100	BASELINE	57.3 ± 6.4%
		Ours(VISION OUTPUT)	60.7 ± 5.4%
		Ours(LSTM OUTPUT)	60.7 ± 5.7%
	500	BASELINE	58.1 ± 4.8%
		Ours(VISION OUTPUT)	61.4 ± 3.8%
		Ours(LSTM OUTPUT)	61.7 ± 3.9%

^aTraining steps per epoch.

outputs and LSTM outputs (59.4% vs 59.2%, 63.1% vs 62.9%, 60.7% vs 60.7% and 61.4% vs 61.7%) for our proposed method.

It is also noted that for both methods, accuracy performance can be improved with the increased number of training steps per epoch, which is within our expectation since more steps means more data augmentation. The best performance in our performed experiments is 63.1% for our proposed method and 59.5% for the baseline method, both of which are using GoogleNet Inception v3 pretrained on ImageNet with 500 training steps per epoch, and the confusion matrices are given in Figure 3. We believe that there is still room for performance improvement on this particular diabetic retinopathy problem by doing more data augmentation, using oversampling instead of undersampling (i.e. to make full use of images in the dataset), and using the original high resolution images. However, the purpose of this paper is to present and validate the idea of disease progression learning, and we leave the optimization for our next study.

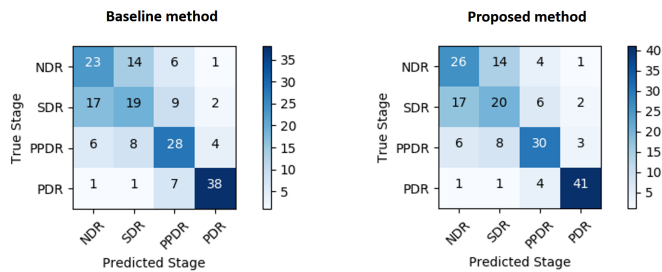


Fig. 3. Confusion matrices of the baseline method (left) and our proposed method (right) using GoogleNet as the vision model with 500 training steps per epoch.

4 Conclusion

In this paper, we present a novel method for medical image recognition by leveraging disease progression learning, where stage sequences are learned by LSTM after feature extraction with a shared vision model for the images from each stage. Compared to the baseline method that is a pure vision model, our proposed method has an average of 3.3% accuracy increase based on our performed experiments, when evaluated for the problem of disease staging on a diabetic retinopathy dataset.

References

1. Litjens, G., Kooi, T., Bejnordi, B.E., Setio, A.A.A., et al.: A survey on deep learning in medical image analysis. *Medical image analysis* 42, 60–88 (2017)
2. Huang, X., Shan, J., Vaidya, V.: Lung nodule detection in CT using 3D convolutional neural networks. In: *ISBI* (2017)
3. Kawahara, J., Brown, C.J., Miller, S.P., Booth, B.G., Chau, V., et al.: Brain-NetCNN: convolutional neural networks for brain networks; towards predicting neurodevelopment. *NeuroImage* 146, 1038–1049 (2017)
4. Nie, D., Zhang, H., Adeli, E., Liu, L., Shen, D.: 3D deep learning for multi-modal imaging-guided survival time prediction of brain tumor patients. In: *MICCAI*. pp. 212–220. Springer (2016)
5. Burstein, H.J., Polyak, K., Wong, J.S., Lester, S.C., Kaelin, C.M.: Ductal carcinoma in situ of the breast. *NEJM* 350(14), 1430–1441 (2004)
6. Inzitari, D., Pracucci, G., Poggesi, A., Carlucci, G., Barkhof, F., et al.: Changes in white matter as determinant of global functional decline in older independent outpatients: three year follow-up of LADIS (leukoaraiosis and disability) study cohort. *BMJ* 339, b2477 (2009)
7. Takahashi, H., Tampo, H., Arai, Y., Inoue, Y., Kawashima, H.: Applying artificial intelligence to disease staging: Deep learning for improved staging of diabetic retinopathy. *PloS one* 12(6), e0179790 (2017)
8. Hochreiter, S., Schmidhuber, J.: Long short-term memory. *Neural computation* 9(8), 1735–1780 (1997)
9. Zhang, Z., Xie, Y., Xing, F., McGough, M., Yang, L.: Mdnnet: A semantically and visually interpretable medical image diagnosis network. In: *CVPR* (2017)
10. Lipton, Z.C., Kale, D.C., Elkan, C., Wetzell, R.: Learning to diagnose with LSTM recurrent neural networks. *arXiv preprint arXiv:1511.03677* (2015)
11. Pham, T., Tran, T., Phung, D., Venkatesh, S.: Deepcare: A deep dynamic memory model for predictive medicine. In: *Pacific-Asia Conference on Knowledge Discovery and Data Mining*. pp. 30–41. Springer (2016)
12. Choi, E., Bahadori, M.T., Schuetz, A., Stewart, W.F., Sun, J.: Doctor AI: Predicting clinical events via recurrent neural networks. In: *Machine Learning for Healthcare Conference*. pp. 301–318 (2016)
13. Chen, J., Yang, L., Zhang, Y., Alber, M., Chen, D.Z.: Combining fully convolutional and recurrent neural networks for 3D biomedical image segmentation. In: *NIPS*. pp. 3036–3044 (2016)
14. Xue, W., Lum, A., Mercado, A., Landis, M., Warrington, J., Li, S.: Full quantification of left ventricle via deep multitask learning network respecting intra- and inter-task relatedness. In: *MICCAI*. pp. 276–284. Springer (2017)